AD-A074 177 TEXAS TECH UNIV LUBBOCK DEPT OF CHEMISTRY F/G 11/9
STUDIES OF HNFN OLIGOMERIC SPECIES.(U)
JUL 79 R L REDINGTON AFOSR-78-3616
UNCLASSIFIED AFOSR-TR-79-0950 NL

END
DATE FILMED
10-79
DDC

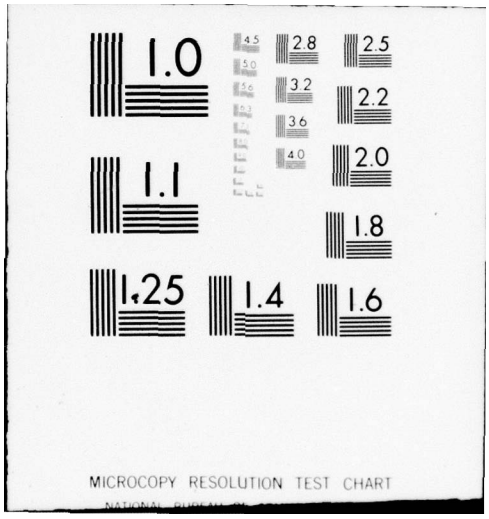
1.0
1.1
1.25
1.4
1.6
1.8
2.0
2.2
2.5
2.8
3.2
3.6
4.0
4.5
5.0
5.6
6.3
MICROCOPY RESOLUTION TEST CHART

AFOSR-TR- 79-0950

FINAL REPORT

1 Jun 78 - 31 May 79

"STUDIES OF H_nF_n OLIGOMERIC SPECIES"

AFOSR — 78 —3616.

1 June 1978 - 31 May 1979

Richard L. Redington
Department of Chemistry
Texas Tech University
Lubbock, TX 79409

2302
D9
40p.

27 July 27, 1979

REPORT DOCUMENTATION PAGE	READ INSTRUCTIONS BEFORE COMPLETING FORM
1. REPORT NUMBER: AFOSR-TR-79-0950 / 2. GOVT ACCESSION NO.	3. RECIPIENT'S CATALOG NUMBER
4. TITLE (and Subtitle): STUDIES OF H_nF_n OLIGOMERIC SPECIES	5. TYPE OF REPORT & PERIOD COVERED: Final report, 1978 June 01-1979 May 31
	6. PERFORMING ORG. REPORT NUMBER
7. AUTHOR(s): Richard L. Redington	8. CONTRACT OR GRANT NUMBER(s): AFOSR-78-3616 New
9. PERFORMING ORGANIZATION NAME AND ADDRESS: Department of Chemistry, Texas Tech University, Lubbock, TX 79409	10. PROGRAM ELEMENT, PROJECT, TASK AREA & WORK UNIT NUMBERS: 2302/D9
11. CONTROLLING OFFICE NAME AND ADDRESS: AF Office of Scientific Research/NC, Building 410, Bolling AFB, DC 20332	12. REPORT DATE: 26 July 1979 13. NUMBER OF PAGES: 39
14. MONITORING AGENCY NAME & ADDRESS (if different from Controlling Office)	15. SECURITY CLASS. (of this report): Unclassified 15a. DECLASSIFICATION/DOWNGRADING SCHEDULE

16. DISTRIBUTION STATEMENT (of this Report)

Approved for public release; distribution unlimited

17. DISTRIBUTION STATEMENT (of the abstract entered in Block 20, if different from Report)

18. SUPPLEMENTARY NOTES

19. KEY WORDS (Continue on reverse side if necessary and identify by block number)

matrix-isolation
hydrogen fluoride
oligomer
dimer
infrared
vibration
spectroscopy
nonideal gas
STO-3G

20. ABSTRACT (Continue on reverse side if necessary and identify by block number)

Separate sheet

DD FORM 1 JAN 73 1473 EDITION OF 1 NOV 65 IS OBSOLETE

SECURITY CLASSIFICATION OF THIS PAGE (When Data Entered)

STUDIES OF H_nF_n OLIGOMERIC SPECIES

Abstract

Infrared matirx-isolation spectra of HF and HF/H_2O mixtures suspended in solid argon have been obtained in the range 400-4000 cm^{-1}. Bands attributed to HF and to HF-H_2O oligomers were observed. HF stretching modes were assigned to dimer, chain trimer, cyclic tetramer, and cyclic hexamer of HF. Some of the FH· · ·F angle deformation modes were observed for these molecules. The oligomers are formed during matrix deposition and the chain trimers appear to be matrix stabilized in a double substitution site in argon. Application of a non-ideal gas model to the literature vapor phase data on HF suggests that the dimer and the hexamer are the dominant vapor phase oligomers, with the hexamer most important near saturation vapor pressures. The tetramer is the next most important vapor phase oligomer, but it contributes only weakly to the vapor phase properties. Minimal basis set STO-3G computations on chain and cyclic HF trimer and tetramer molecules suggest the marked increase in stability that arises on catenation or (unstrained) cyclization of HF systems.

STUDIES OF H_nF_n OLIGOMERIC SPECIES

I. RESEARCH OBJECTIVES

It was proposed to use matrix-isolation spectroscopy to study the properties and vapor phase populations of oligomers of HF and DF. The properties to be determined included the existence of specific oligomers, their molecular symmetry and qualitative geometry, their vibrational frequencies, and at least a partial analysis of their molecular force fields. The research effort was designed to provide information concerning intermolecular interactions between HF molecules and, thereby, to provide information that is useful for modeling collisions and intermolecular energy transfer in the HF vapor. Accurate models to describe collisional relaxation processes involving monomer-monomer collisions or monomer-oligomer collisions are essential for providing quantitative kinetic models for HF or DF lasers. These lasers are useful for Air Force operations involving reconnaissance, communication, detection, surveillance, and weaponry.

II. STATUS OF RESEARCH EFFORT

A. Matrix-Isolation Experiments

Hydrogen fluoride has been studied using matrix-isolation sampling several times previously (1,2,3) but the research effort was directed at investigating the behavior of matrix-isolated HF monomer rather than at elucidating properties of H_nF_n oligomers. The matrix-isolated HF monomer is of interest because it undergoes hindered rotation in rare gas lattice trapping sites. Rotation is suggested by observations on several bands attributed to vibration-rotation transitions, and this phenomenon is consistent with results obtained on several other small molecules that are capable of fitting into substitutional trapping sites in the rare gas lattices, e.g. H_2O(4), NH_3(5), HCl(6), CH_4(7).

The only published spectra that pertain to H_nF_n oligomers are shown in reference 1, but the HF samples shown there are contaminated with large quantities of water, and many of the observed absorptions are evidently due to $(H_2O)_n$ and complexes between HF and H_2O rather than to H_nF_n oligomers. The spectra obtained in the present research differ significantly from these results, as water and other impurity molecules are nearly all eliminated. In contrast to the status concerning matrix-isolated H_nF_n oligomers, rather complete studies have been reported for hydrogen chloride oligomers(8) and for water oligomers(9).

EXPERIMENTAL TECHNIQUE. The matrix-isolation technique consists of trapping the sample molecules in a large (hundreds-fold or thousands-fold) excess of inert matrix material. In the present research the matrix material was exclusively argon. Neon is probably a better matrix choice; however, neon could not be used with the available low temperature refrigerator. The inert matrix interacts little with the isolated sample molecules, which therefore exhibit near-vapor phase vibrational band origins. The absorption peaks are sharp due to the absence of a rotational band envelope or to strong intermolecular interactions. The rigid matrix prevents coalescence of smaller species to form solid HF.

In "premixed" experiments the gaseous HF and Ar are mixed together in a sample cylinder at (nominally) known pressures. The gaseous mixture is then sprayed onto the cold (11 K) sample holder, where it freezes into a rigid solid. In the case of HF, accurate knowledge of the M/S (matrix to sample) ratios seems precluded in the work performed to date because the HF is strongly adsorbed onto the walls of the sample cylinder and, moreover, it tends to react with these walls to form SiF_4 (stainless steel contains small amounts of Si, which the HF manages to reach).

In this research two types of matrix-isolation sample preparations have been performed. These are the "premixed" vapor deposition just described and a

"pin hole" or double jet deposition technique. In the latter, the HF vapor source is thermostatted at constant pressure (the present range of interest is less than one atmosphere) and then it is allowed to escape into the cryostat system through a tiny orifice. The effusing HF beam is codeposited with an argon beam on the cold sample holder. The objective of such double jet experiments is to obtain reliable spectra of the oligomers present in the original HF vapor at known temperature and pressure. In premixed sample preparations the HF partial pressure is too low to allow the presence of vapor phase oligomers and they are formed in the matrix-isolation samples upon deposition by coalescence of monomers brought together--using concentrated M/S ratios. On the other hand, hexamers and other oligomers can, in principle, be directly obtained from HF vapor at very dilute M/S ratios using the double jet deposition system. Ideally, their absorption intensities will reflect the original HF vapor phase composition.

In the present deposition system, the pin hole is an orifice laser drilled(10) at the apex of a cone bored into the outer end face of a standard Gyrolok 1/4 inch tube cap. Orifice diameters of 0.005 to 0.0005 inch were prepared. A dozen experiments were performed using double jet deposition, with results that differ markedly from those obtained using standard premixed samples, but it does not appear that these matrix-isolation samples reflect the vapor compositions of the original vapor. There are still experimental problems associated with perfecting the double jet apparatus but one difficulty may be the pinhole orifice itself. A more appropriate construction is to drill the pin hole into a cap of very thin foil, thus avoiding the presence of a volume where collisional relaxation and partial low pressure equilibration can occur. The spectra to date reflect a lower oligomer composition than expected from the original HF gas sample.

It was originally intended to construct an all monel vacuum system for the

HF purification and sample preparation. The present system includes monel tubing, fittings, and valves, but also stainless steel valves and a 0.5 l stainless steel sample preparation cylinder. We were forced to wait nine months for the sample preparation cylinder and nearly as long for some of the other components. The sample cylinder is the essential component of the "premixed" matrix-isolation experiments and, in spite of repeated serious attempts, satisfactory experiments were not possible until the high quality stainless steel vessel was finally delivered. The earlier experiments used a Teflon plastic gas sampling bag, which leaked, a metal storage cylinder already present in the laboratory, which reacted with HF to yield numerous unknown impurities, and a locally constructed stainless steel cylinder, which reacted with the HF to yield objectionably large amounts of SiF_4. At present we have saved spectral charts for above forty numbered matrix-isolation experiments (including some poor ones). These experiments are for HF premixed with Ar at various matrix/sample ratios nominally ranging from about 30 to several hundred, pin hole deposits, and a series of experiments for HF/Ar with water (O-16 and some with O-18) added in order to study the spectra of the HF-H_2O complexes as well as the H_nF_n oligomers. The HF gas was purchased from Matheson Company and purified for each experiment by pumping on samples trapped at 77 K and then at about 185 K. A partial spectral analysis has been performed on the available data, as discussed below, but before publication additional, confirmatory experiments using deuterated molecules, and water O-18 will be performed. Those will allow force field calculations to be performed in some cases. The experiments are presently being performed without AFOSR aupport.

The research is performed using an Air Products Displex Model 202 closed cycle low temperature refrigerator rather than the liquid helium cryostat. This is economical and allows the use of an argon matrix, but is not cold enough for

a neon matrix. A Beckman IR-9 spectrophotometer is used to record the spectra in the range 400-4000cm^{-1}. We hope to perform experiments in the spectral range below 400 cm^{-1} using a Beckman IR-11 far-infrared spectrometer that is available in this laboratory.

RESULTS. The argon matrix-isolation spectra show intense absorptions in the spectral region between 3000-4000 cm^{-1} that are due to HF stretching modes, and generally weaker absorptions (with two exceptions) in the region 400-800 cm^{-1} that are due to bending or angle deformation modes. The region above 3700 cm^{-1} shows four intense absorptions attributed to oligomers, along with a number of weaker bands. The lower frequency region shows surprisingly few absorptions. Representative spectra are shown in Fig. 1 and the absorptions are listed, along with those of previous investigations, in Table I. These results are discussed according to the various oligomers in the following paragraphs.

Monomer. The present experiments were not designed to study the monomer spectrum which, as mentioned, is of interest in terms of hindered rotation of HF in the rare gas matrix environment. The monomer absorptions consist of a very intense doublet and two very weak side bands. The weak side bands were not observed in the present work. The intense doublet closely resembles that illustrated by Mason, Von Holle and Robinson(3), with components of rather similar intensity and not well resolved. The slightly more intense, higher frequency component has been attributed to R(0) of the rotating monomer; the lower frequency component attributed to HF in a different matrix trapping site.

Dimer. The approximate geometry of the dimer is known from microwave and radiofrequency studies by Dyke, Howard and Klemperer(11) using molecular beam samples. The dimer has the geometry

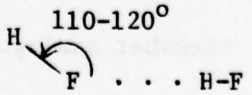

FF = 27.9 nm
FH = 9.2 nm.

This tetratomic molecule possesses six infrared active vibration frequencies, but

the only previous experimental observations consist of the measurement of weak infrared absorption that occurs between several of the intense, low J, vibration-rotation bands of the gaseous monomer. This absorption has been studied by Smith(12), Herget, Gailar, Lovell and Nielsen(13), and Himes and Wiggins(14). The absorption profile is poorly characterized because of experimental difficulties, but there appear to be three maxima and fine structure is resolved over portions of the profile. There is an intense band in the argon matrix at 3881 cm^{-1} that corresponds reasonably well with the center of the complex vapor phase dimer absorption. The argon matrix band is assigned to dimer because it is the last oligomer absorption to persist at dilute M/S ratios, while Smith(12) assigns the vapor phase absorption to dimer because its intensity shows a P^2 pressure dependence.

The vibrational band origin may be taken to be near the 3881 cm^{-1} argon matrix value. The other "bands" observed in the vapor phase are either hot bands or else part of a complex profile associated with the 3881 cm^{-1} fundamental. The presence of a complex absorption profile, in contrast to that of a conventional near-symmetric top (cf. Ueda and Shimanouchi(15)), is consistent with the available knowledge of the dimer. The microwave spectra(11) show complexity suggesting that the molecule is nonrigid and that tunneling of the H atoms occurs:

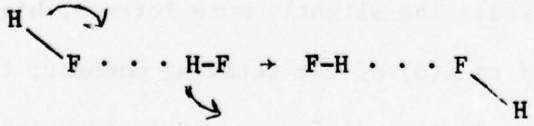

Experience with other nonrigid molecules has illustrated the complexity that arises in their vapor phase infrared spectra. For example, carbon suboxide is a quasilinear molecule with a very low frequency, large amplitude C=C=C angle bending mode that is somewhat analogous to the rocking of the "free" HF moiety of the H_2F_2 dimer. The appearance of the C_3O_2 low resolution spectrum is deceptive(16), as made obvious by later high resolution studies(17), and it is only

recently that the analysis of the potential function and intramolecular dynamics are becoming understood(18). Likewise, OH stretching modes of hydrogen bonded carboxylic acid dimers have enormously broad, complex band contours, even in a neon matrix(19), due to intramolecular interactions involving the hydrogen bond linkages(20). The extreme band broadness and intensification caused by H-bonding in the carboxylic acid dimers is not shown by H_2F_2 dimer in the vapor or in the argon matrix, but it is present in solid HF where large scale intermolecular couplings can occur. This is analogous to the case for water.

The second HF stretching mode is much less intense than the 3881 cm^{-1} band, and considerations of the overall matrix-isolation data that are presently available suggests that the best choice is a band at 3787 cm^{-1}. The intensity of this band correlates better with that of 3881 than do intensities of the other possible candidates. Unfortunately, it appears that matrix conditions strongly affect the intensity of the various H_nF_n oligomer transitions. This is undoubtedly because of the great flexibility of the oligomer molecules, and it provides a problem because a precise correlation of the band intensities with relative populations is precluded as M/S ratios are varied. However, relative correlations are still possible in many cases, as shown by plotting relative intensities against matrix dilutions.

Assigning the 3787 cm^{-1} band as the second HF stretching mode of the dimer is in accord with published ab initio quantum mechanical calculations(21). These place the two HF stretches only 43 cm^{-1} apart (at 4081 and 4038 cm^{-1}) although they are about 200 cm^{-1} higher than the observed values. In spite of the hydrogen bond, the two HF stretches have nearly the same vibrational frequencies, and they can be expected to strongly couple. Because of its greater intensity the 3881 cm^{-1} band must correspond approximately to an "in-phase" motion of the two HF vibrators, while the weaker 3787 cm^{-1} band must correspond to "out-of-phase"

motion. The lower frequency mode has a larger contribution from the H-bonded HF moiety but, as noted, it does not show the large intensification and enormous frequency shift associated with some H-bonded stretching modes.

Two bending modes of the dimer correspond roughly to in-plane and out-of-plane motion of the H-bonded (F···HF) H atom. These modes are calculated quantum mechanically to occur at 588 cm^{-1} (in-plane) and 519 cm^{-1} (out-of-plane) but no experimental measurements exist. These two bending modes are evidently very weak and/or broadened in the argon matrix isolation spectra as no absorptions positively assignable to the dimer have yet been identified outside the HF stretching spectral region. The tendency for the dimer H atoms to tunnel and the overall molecular flexibility evidently affect the appearance of the bending transitions, most likely broadening them. This type of behavior was recently observed for certain vibrational modes of tropolone(22), where sharp bands were observed upon deuteration of the labile H atom and a neon matrix, which is less interactive than argon was used. The two lowest frequency vibrational modes of the dimer are the F···F stretch and a rocking of the free HF moiety. Both of these frequencies are expected to fall below the range of the presently observed spectral region. They are calculated(21) to occur at 226 and 171 cm^{-1}.

Trimer. No experimental evidence for the existence of the H_3F_3 trimer is present in the literature. The various studies (vida infra for discussion) indicate that the dimer, tetramer, and hexamer have greater stability in the vapor phase. However, trimer can exist in vapor, as suggested by the mass spectrometric observation of a (nonpolar) ion containing three F atoms(11).

The matrix-isolation experiments show the presence of four intense oligomer absorptions in the HF stretching region. The 3881 cm^{-1} band is due to dimer and the other three bands are therefore due to higher oligomer(s). Their intensities do not correlate precisely with M/S ratio, but the 3826 cm^{-1} and 3702 cm^{-1} bands

are very closely associated as shown, for example, by their parallel behavior in the presence of SiF_4 impurity. Plots of the three band intensities, scaled relative to the normalized 3881 cm^{-1} dimer band, show that all three increase relative to the dimer band (but not by the same amount) as the M/S ratio is made more concentrated. All three bands are assigned to the chain trimer in preference to including cyclic trimer or higher oligomers. The chain trimer is chosen because it has three infrared active HF stretching modes, the intensities of the three observed bands correlate reasonably well together, and because they occur in the spectral region of the (chain) dimer HF stretching modes. There is a gap in the appearance of the intense HF stretching modes in the argon matrix spectra that strongly suggests the presence of chain dimer and trimer with absorptions in the range 3702-3920 cm^{-1}, and other oligomers with HF stretching absorptions in the range below 3430 cm^{-1}. It is known that cyclic hexamer and (probably cyclic) tetramer have their single infrared allowed mode in the latter region(23) and that the long chain (solid) HF system also absorbs there(24). The chain trimer fits very well into a double substitutional site in solid argon. Matrix warmup studies suggest that it is matrix stabilized in its trapping site, as the sharp trimer absorption bands persist while absorptions due to other species disappear. This type of behavior has also been observed for Li_nF_n oligomers(25).

Several weak absorptions are observed in the HF stretching region above 3700 cm^{-1} that may be associated with chain oligomers longer than trimer. All n HF vibrations of the chain oligomers are infrared active, in contrast with the single allowed mode of the planar, cyclic molecules.

The chain trimer possesses four FH· · ·F bending modes. Assuming linear hydrogen bonds, which define a plane, the in-phase, out-of-plane mode should be intense while the out-of-phase mode should be weaker. The two in-plane modes

should be far less affected by tunneling and, therefore, nonrigidity than is the corresponding dimer mode since tunneling involves motion by three H atoms rather than two. In contrast with the unobserved dimer vibrations, intense trimer bands attributed to FH· · ·F bending modes are observed at 446 and 561 cm^{-1}.

The remaining five chain trimer modes (two F· · ·F stretches, two "rocking" modes, and one torsion) are all expected to fall below 400 cm^{-1}.

Hexamer and Tetramer. The H_6F_6 hexamer is known to exist abundantly in the vapor at pressures approaching saturation (see discussion in the next section), but it is most likely not present in the low pressure HF vapor deposited in premixed matrix-isolation samples. Electron diffraction studies(26) show that the hexamer is cyclic; however, it is not positive that the molecule is planar. Very likely it is planar with large amplitude angle bending vibrations, but the possibility for boat or chair equilibrium configurations also exists(26).

A planar cyclic hexamer (symmetry group C_{6h}) and tetramer (C_{4h}) each have only four infrared active vibrations. These are an HF stretch, an in-plane and an out-of-plane angle deformation, and a low-frequency F· · ·F stretch. Spectral studies by Smith(23) yield rather approximate values for the overlapped, infrared active HF stretches in the vapor. He gives derived band profiles with maxima near 3350 and 3500 cm^{-1}, respectively, for hexamer and tetramer. The absorption is assigned to these oligomers on the basis of its temperature and pressure dependence. Smith reports additional absorption near 1200 and 700-850 cm^{-1} for hexamer and near 700 cm^{-1} for tetramer. The argon matrix-isolation results have not yet been completed on these oligomers because the double jet deposition experiments have not been perfected. Nevertheless, bands due to HF oligomers occur at 3430 cm^{-1} and 3250 cm^{-1} which are very likely due to the tetramer and hexamer because of their proximity to the estimated vapor phase values. These bands grow on diffusing dilute matrix-isolation samples, and occur only for initial deposits

with concentrated M/S ratios.

The relative sparcity of bands in the FH· · ·F deformation region, as well as in the HF stretching region, corroborates the idea that the larger oligomers of HF are cyclic and symmetric rather than chains and asymmetric. The 1200 cm^{-1} absorption reported by Smith for the vapor phase hexamer was not clearly observed in the present experiments; frequencies proposed for the single infrared active angle deformation modes of the tetramer and hexamer are listed in the Tables.

Hydrogen Fluoride - Water Complexes. The FH· · ·OH_2 dimer has been studied by microwave spectroscopy(27), infrared spectroscopy(28), and ab initio quantum mechanics(29). The structure is analogous to the H_2F_2 dimer, with a roughly linear FH· · ·O linkage but it has not been established that it is a nonplanar molecule. The published infrared spectra(28) are rather incomplete, with only the direct observation of a broad vapor phase band extending downwards in frequency from about 3600 cm^{-1} and another broad band near 650 cm^{-1}. Hot bands are superposed on these absorptions, and Thomas(28) interprets the peaks in a manner leading to values for four fundamental bending modes. No information exists concerning higher oligomers.

Argon matrix-isolation experiments using HF and H_2O mixtures yield absorptions clearly due to complexes. The available data suggest that a trimolecular complex containing two HF molecules and one H_2O is particularly stable in the argon matrix. A strong absorption band at 3554 cm^{-1} grows into the spectrum and the 3881 cm^{-1} H_2F_2 dimer band concomitantly disappears on concentrating H_2O in the matrix. The 3554 cm^{-1} frequency is significantly lower than the 3608 cm^{-1} vapor phase value given for the FH· · ·OH_2 dimer(28), whereas the vapor phase and argon matrix frequency values for the corresponding HF· · ·HF vibration agree well. On reviewing the argon matrix data, it appears that the FH· · ·FH· · ·OH_2 molecules, likewise, behave similarly. The dimer spectra are weak in relatively concentrated matrices, while the trimer spectra show several very intense bands. The trimer

molecules both fit double substitutional sites in argon and warmup studies suggest that both are matrix-stabilized. The second HF stretching mode of the mixed $(HF)_2OH_2$ trimer is weak as it is basically an antisymmetric combination of the two HF oscillators. All three "H_2O" modes are weak in its complexes, and other research shows they are not shifted much in frequency from the monomeric H_2O values(9,30).

Four bands appear just below 650 cm^{-1} in the FH· · ·F angle deformation region. These bending modes, which are assigned in the Tables, are higher in frequency than those of the ClH· · ·OH_2 dimer(30) but close to the vapor phase frequencies given for FH· · ·OH_2 dimer by Thomas(28).

B. Composition of Hydrogen Fluoride Vapor

It is well known that at modest temperatures HF vapor is highly associated at pressures extending considerably below its saturation vapor pressure. In contrast to most other substances, hydrogen fluoride has a tendency to form hydrogen bonded vapor phase oligomers, rather than to immediately condense to form the liquid. In addition to association, it is expected that the strong attractive forces existing between HF molecules should lead to significant nonideality of the vapor. An attempt is made here to provide a unified model for the HF vapor by introducing gas nonideality in the form of a virial coefficient. The nonideality contribution nearly vanishes for low pressure, high temperature data sets, but plays an important role for data sets obtained at pressures near saturation. It seems impossible to precisely represent the complex overall experimental phenomena observed for HF vapor in terms of very few adjustable parameters; however, a moderately successful attempt is made to reconcile the vapor density data, specific heat data, infrared spectroscopic data, and third law entropy data in terms of one or two adjustable gas nonideality parameters and two or three equili-

brium constants.

The density of HF vapor was analyzed in terms of a monomer-hexamer equilibrium many years ago(31). Saturated and near saturated vapor yields a linear van't Hoff plot over a 100°C temperature range(31,32) for the hexamerization reaction 6 HF $\rightleftarrows$ H_6F_6. It therefore appears as a consequence that any model for HF vapor composition must lead to hexamer as the dominant oligomer along the saturation vapor pressure line. Careful analysis by Maclean, Rossotti and Rossotti(34), hereafter MRR, of highly accurate vapor density data obtained by Strohmeier and Briegleb(33), suggests that a monomer-dimer-hexamer equilibrium fits the data best. The data covers pressure ranges that are considerably below the saturation values, and the data fit involves only low pressures of dimer and hexamer. The MRR analysis is based on ideal gas behavior and the model fails to reproduce the vapor density data as pressure increases and oligomer concentrations rise to high levels. Extrapolation of their results to the saturation vapor pressure predicts association factors Z(Z = apparent molecular weight of associated vapor divided by molecular weight of monomer) that are far below those observed(32) for the saturated vapor.

Infrared spectral studies of HF vapor by Smith(12,23) suggest that dimer, tetramer, and hexamer are all present in HF vapor in the P-T regime investigated by Strohmeier and Briegleb(33). The infrared results suggest that the tetramer and hexamer have large absorption coefficients and that these molecules are easily detected under P-V-T conditions where their presence has little or no effect on vapor density measurements. The hexamer, for example, shows an intense infrared absorption at -77°C at a total HF pressure of only 2-3 torr(23).

Third law entropy measurements(35) of the saturated vapor strongly reflect molecular association. On using the association factor Z that is obtained from vapor density measurements, a monomer-hexamer model fails to account for the entropy by about 40 J/mol·deg (the calculated vapor entropy is far below that

of the liquid!); therefore, the original analysis of the entropy data used an extended oligomer model(35).

Vapor phase heat capacity measurements(36) show enormous maxima that roughly parallel the saturation pressure curve. The maxima are unexcelled among vapor phase heat capacities, and arise because of the enthalpies of the various oligomerization reactions. The C_p curves are dominated by a monomer-cyclic hexamer equilibrium, but a more quantitative fit is obtained upon introducing a vapor model including a series of chain oligomers(36).

In general, each data set has been analyzed in terms of a specific vapor model and the various models are not consistent with one another. However, it is apparent that the entropy and heat capacity data can be approximately fitted by a monomer-dimer-hexamer model if the K_6 equilibrium constant is lowered from that calculated using the observed saturated vapor density data. Adjustment of K_2 and K_6 to fit more extensive data is accomplished by introducing nonideal gas behavior as described below. Maclean, Rossotti and Rossotti(34) found minimal evidence for any single additional oligomer beyond dimer and hexamer, although (obviously) an exact data fit can be accomplished by adding several oligomers because of the rather indeterminate equilibrium constants. Since tetramer was observed at low pressures in the vapor phase infrared measurements along with the hexamer, the present analysis includes dimer, tetramer, and hexamer as the most important oligomer species. The analysis essentially reproduces that of MRR at the ideal gas level, but extension by the introduction of a second virial coefficient leads to calculated values in reasonably close agreement with each of the four different data sets.

In order to orient the P-T regimes of the various data sets relative to one another, they are presented together in Fig. 2. Rather than plotting isotherms of Z versus pressure, a plot of the excess volume versus pressure, as

originally drawn by Vanderzee and Rodenberg(37), is presented. The excess volume, V^E, is simply the difference between the actual volume of one gram formula weight of associated HF vapor and the ideal gas volume. Horizontal isotherms reflect the presence of monomer and dimer, while sharply dipping isotherms reflect the occurrence of higher oligomerizations. Superposed on the excess volume isotherms at appropriate pressures are the infrared and calorimetric measurements, as described in the figure caption.

NONIDEAL VAPOR MODEL. Vapor density data are expressed using the equation of state for one formula weight (20.01 g) of HF as

$$PV = RT/Z \tag{1}$$

This equation is empirical and in the previous work Z was attributed exclusively to molecular association. In the present case it is generalized to

$$Z = Z_A Z_N \tag{2}$$

where Z_A is the equation of state correction due to association and Z_N is that due to gas nonideality (including effects from all vapor phase species). Introducing a similarly comprehensive virial coefficient B, the equation of state is written

$$PV = nRT\ (1 + nB/V) \tag{3}$$

with

$$1/Z = 1/Z_A Z_N = n\ (1 + nB/V). \tag{4}$$

Since $n = 1/Z_A$,

$$\begin{aligned} 1/Z_n &= 1 + nB/V \\ &= 1 + ZBP/RTZ_A \end{aligned} \tag{5}$$

gives the nonideality correction. The second virial coefficient for a gaseous

mixture is written(38)

$$B = \sum_{ij} B_{ij} X_i X_j \qquad (6)$$

where X_i is the mole fraction of the "i"th oligomer, now represented as $H_{n_i} F_{n_i}$. Calculations using simple model potential functions suggest that the second virial coefficient for each type of molecule will be roughly proportional to its volume and, with strong attractive forces, to an exponential term: $\exp(\Delta\varepsilon_{ij}/RT)$, where $\Delta\varepsilon_{ij}$ is the depth of the potential well resulting from interaction between the n_i and n_j oligomers. Because all the B_{ij} virial coefficients cannot be realistically determined for the HF oligomers, simplifying assumptions of the form

$$B_{ij} = \sqrt{F_i F_j}\ B_{11} \qquad (7)$$

were made. The F_i values (excluding F_1, always unity) were assumed to take the forms (A) $F_i = s\, n_i$, or (B) $F_i = s\, n_i^2$, with s a scale factor given the same value for all oligomers. With $F_i = n_i$ the assumption corresponds to saying, for example, that the hexamer is six times as voluminous as the monomer, and that the stronger (rotationally averaged) dipole and hydrogen bonding attractions of the monomer are approximately balanced by the stronger and more orientationally uniform attractive van der Waals forces of the hexamer (i.e. $\Delta\varepsilon_{ii}$ is equal for the two oligomers). For $F_i = n_i^2$ the volume relation is still the same but $\exp(\Delta\varepsilon_{66}/RT)$ is six times greater than $\exp(\Delta\varepsilon_{11}/RT)$. This implies that $(\Delta\varepsilon_{66} - \Delta\varepsilon_{11}) \sim$ 4.7 kJ/mol.

The computations tested assumptions (A) and (B). First, the vapor density data of Briegleb and Strohmeier(33), which is given for five temperatures between 26 and 56°C, was fitted to obtain values for the K_2 and K_6 or the K_2, K_4 and K_6 equilibrium constants as a function of the second virial coefficient B (i.e.

B_{11} and s). Rather than using a graphical method as done by Maclean, Rossotti and Rossotti(34), a simultaneous least squares fit of the vapor density data to the total pressure and to the function

$$A = \sum_i n_i K_i P_1^{n_i} \tag{8}$$

was obtained. The monomer pressure P_1 was obtained by numerical integration of the Bjerrum integral, and the results for B = 0 agreed reasonably well with the results of MRR, as shown in Fig. 3. Unweighted least squares were used to fit the same data points as used by MRR, and a 1/Z weighting was used when the Strohmeier-Briegleb data was supplemented by data listed in the paper of Vanderzee and Rodenburg(37). The latter authors include unpublished data in their comprehensive, and smoothed, compilation of the thermodynamic excess properties of hydrogen fluoride vapor. It must be noted that their recommended values for the association factor Z along the saturation curve differ from those of Jarry and Davis(32) by several percent at 26°C. The 1/Z weighting generally favors the Strohmeier-Briegleb data by a factor of 2 or 3 over data closer to the saturation curve.

The quality of the equilibrium constants and one or two second virial coefficient parameters were then assessed by calculating the oligomerization enthalpies, the third law entropies, and the vapor phase heat capacities. Their recommended values for these quantities are tabulated by Vanderzee and Rodenburg(37).

RESULTS. Since the procedure used is semiempirical it was necessary to perform many trial computations to assess the effectiveness of the various vapor phase models. The results of one of these, which yields rather good results, is given in Figure 3 and Table III. It is a monomer-dimer-tetramer-hexamer model; however, the results are nearly identical to those with tetramer excluded. In general, including tetramer is ineffectual for significantly improving the fit to the low pressure vapor density data, as previously concluded by MRR, and including tetramer to improve the fit to the higher pressure data leads to an improved

overall average fit, but to a significantly poorer fit to the (more reliable) low pressure data.

In the present case, the Strohmeier-Briegleb vapor density data was very closely fitted to obtain K_2, K_4 and K_6 values. The data were fitted using unweighted least-squares, as mentioned above, rather than by the visual curve fitting method of MRR. The two ideal gas fittings are compared in the lower two lines of Fig. 3. The present ΔH_2 value, -32.0 kJ/mole, is slightly higher than MRR's value of -27.2 kJ/mole. The latter is in the range usually quoted for the dimerization energy. The ΔH_6 values are similar, the present ideal gas value being -173 kJ/mole while the MRR value is -169 kJ/mole. ΔH_6 changes very little on introducing gas nonideality; however, for given models ΔH_2 may increase to unreasonable values when the higher pressure vapor density data is fitted. Thus, the present nonideal gas model yields low pressure agreement plus agreement between the calculated and the Jarry-Davis experimental Z values for the top set of points drawn in Fig. 3. Models giving very good fits for the saturation Z values have so far given unsatisfactory fits for the entropy and heat capacity.

The present illustrative nonideal gas model is for case (A) with s = 1, i.e. $F_i = \sqrt{n_i}$. ΔH_2 is kept very near the ideal gas value by adding constant increments of -0.10 and -0.15 to the ideal gas values of -log K_2. The resulting K_4 and K_6 values are those yielding least-squares fits to the low pressure vapor density data with the new K_2 values. A B_{11} value arises for each temperature, but the five B_{11} values can be correlated (or generated) quite well with a two parameter temperature dependent function. The set of equilibrium constants were then used to calculate the results shown in Table III, where it is seen that the third law entropy values are about 2 J/mole·deg too low (rather than 40!), that the C_p values have approximately the correct maximum value, but that they peak slightly too soon. Allowing both B and s to be temperature dependent will improve the fit. The present Z_N fit is best using a point intermediate between the

nonideality shifts of -0.10 and -0.15 that were chosen for illustration and to indicate sensitivity. It is seen that the pressures P_4 and P_6 are of the same order of magnitude in the P-T regime chosen by Smith(23) for his infrared studies, so that it is reasonable that both oligomers were observed. His oligomerization enthalpies are near the presently developed values.

The second virial coefficients represented by the B_{11} values increase reasonably as the temperature is lowered from 56 to 26°C. Before this investigation is completed the value of B_{11} (i.e. the monomer second virial coefficient) will be computed using the program LINEAR obtained from QCPE(39) and the HF monomer-monomer interaction potential function published by Jorgensen and Cournoyer(40).

C. Ab Initio Calculations for H_nF_n Oligomers

In order to augment the infrared experiments, a theoretical study of the higher H_nF_n oligomers has been undertaken. These studies are similar in scope to previous computational research on the H_2F_2 dimer(21,41) and make use of the Gaussian 70 computer program from QCPE(42). With the exception of one short note that considers H_3F_3 trimer(43), there appear to be no published calculations for the higher H_nF_n oligomers.

When completed, the present study will include geometry optimization of the cyclic and chain configurations for the trimer, tetramer, pentamer and hexamer. Since the results are dependent on the basis set, the optimum geometry will be calculated using both minimal and split valence basis sets. The analysis includes a calculation of force constants and vibrational frequencies. The geometry optimization utilizes the algorithm of Payne(44). At present, minimal basis set (STO-3G) calculations for the chain and cyclic trimer and tetramer are reported. In each case the oligomer was considered as one molecule and the total energy was minimized with respect to all of the geometrical parameters.

Trimer. Three parameters are necessary to describe the geometry of the planar, cyclic trimer: the F-F bond length, the F-H bond length, and the angle between FH and FF bonds, called α. The cyclic trimer was first assumed to be planar and to have a C_3 axis in order to optimize the bond lengths and α. Planarity was confirmed by calculating energies for rotation of the protons out of the plane into both staggered and symmetrical configurations. The optimized geometrical parameters, a figure giving coordinate definitions, and the total energy are given in Table IV. Likewise, the chain trimer was initially assumed to be planar and the five bond lengths optimized together and the four in-plane angles optimized together. Planarity was confirmed by energy calculations with H atoms moved out of the plane. The energy was lowest for the planar configuration given in Table IV. The barrier hindering rotation of the "free" H atom about the adjacent H· · ·F axis is about 3 kJ.

The interaction energies were obtained using monomer and dimer energies already given by Curtiss and Pople(21). They calculated a total energy of -98.57285 hartrees for the monomer with an HF distance of 9.56 nm using an STO-3G basis set. For the dimer, the HF distances are 9.54 and 9.53 nm with an energy of -197.15447 hartrees. These values yield an interaction energy of -70.5 kJ, or -23.5 kJ per hydrogen bond, when three monomers combine to give the cyclic trimer. The interaction energy of a monomer and dimer to form cyclic trimer is -47.4 kJ or -23.7 kJ per hydrogen bond formed. Corresponding values for the chain trimer are -48.5 kJ and -25.4 kJ. At -24,3 and -25.4 kJ, the STO-3G calculation suggests slightly stronger hydrogen bonds for the chain trimer, but the cyclic trimer would be more stable due to the extra hydrogen bond.

Tetramer. Like the planar cyclic trimer, only three geometrical parameters are required for cyclic tetramer. This molecule was initially assumed to be planar

and the two bond lengths and angle α were optimized. Then, planarity was confirmed as the H atoms were rotated out of the plane in both staggered and symmetrical configurations. Optimized values for the parameters and the total energy are listed in Table IV. The binding energy of four monomers to give the cyclic tetramer is -185.3 kJ or -46.7 kJ per hydrogen bond. This value appears to be much too high, just as the FF bond distance appears too short. Results of the calculations on the chain tetramer are included in Table IV, where they may be compared with the chain trimer.

The minimal STO-3G basis set calculations suggest that the cyclic trimer and tetramer are more stable than the chain forms. Experimentally, the chain trimer appears to be the more stable in an argon matrix, perhaps because of stabilizing matrix interactions. It is premature to discuss the present results in detail in view of the expected limitations of the minimal basis set; however, they certainly anticipate the stronger hydrogen bonding that arises for the cyclic hexamer and long chains of the solid. As pointed out above, there is a gap in the frequency range of the HF stretches for short chains and for the cyclic and long chain systems. In addition, there is a pronounced shortening in the experimental FF bond lengths as seen on comparing the dimer, 27.9 nm(11), cyclic hexamer, 25.5 nm(26), and solid, 24.9 nm(45). Of course, the unstrained cyclic systems have properties in common with the infinite chain.

One objective in performing the ab initio calculations is to assist in the vibrational analysis of the observed spectra by providing relative ranges and frequency orderings for the various oligomers.

D. Summary of Results

1. Infrared spectra of several HF and HF/H_2O mixtures suspended in solid argon were obtained in the range 400-4000 cm^{-1}.

2. The data show HF stretching bands attributed to monomer, chain dimer, chain trimer, cyclic tetramer and cyclic hexamer. The data show FH· · ·H angle deformation modes attributed to these same oligomers; however, not all of the anticipated bending frequencies were located (in particular, the dimer bending modes are not listed).

3. There seems to be parallel behavior for the dimers FH· · ·FH and FH· · ·FH· · ·OH_2. The trimer molecules appear to be stabilized in the argon matrix, and to possess some very intense, sharp absorptions.

4. The dominant oligomers in HF vapor appear to be the dimer and the hexamer. The latter molecule is very important as saturation vapor pressures are approached. The next most important oligomer is the tetramer, although it plays a very minor role. These conclusions are suggested by a literature review and by application of a nonideal gas model to vapor phase density, third law entropy, heat capacity, and infrared spectral data.

5. There appears to be stabilization of the FH· · ·F hydrogen bonds on catenation or on unstrained cyclization of HF systems. Minimal basis STO-3G calculations on various oligomers suggest this trend, which is apparent in the experimental data.

E. References

1. M. T. Bowers, G. I. Kerley and W. H. Flygare, J. Chem. Phys., 45, 3399 (1966).
2. D. W. Robinson and W. G. Von Holle, J. Chem. Phys., 44, 410 (1966).
3. M. G. Mason, W. G. Von Holle and D. W. Robinson, J. Chem. Phys., 54, 3491 (1971).
4. R. L. Redington and D. E. Milligan, J. Chem. Phys., 39, 1276 (1963).
5. L. Abouaf-Marguin, M. E. Jaycox and D. E. Milligan, J. Molec. Spectrosc., 67, 34 (1977).
6. L. F. Keyser and G. W. Robinson, J. Chem. Phys., 44, 3225 (1966).

7. A. Cabana, G. B. Savitsky and D. F. Hornig, J. Chem. Phys., 39, 2942 (1963).

8. L.-C. Brunel, J.-C. Bureau and M. Peyron, Chem. Phys., 28, 387 (1978).

9. G. P. Ayers and A. D. E. Pullin, Spectrochim. Acta, 32A, 1689 (1976); L. Fredin, B. Nelander and G. Ribbegard, J. Chem. Phys., 66, 4065 (1977).

10. Precision Aperture, Fort Wayne, Indiana

11. T. R. Dyke, B. J. Howard and W. Klemperer, J. Chem. Phys., 56, 2442 (1972).

12. D. F. Smith, J. Molec. Spectrosc., 3, 473 (1959).

13. W. F. Herget, N. M. Gailar, R. J. Lovell and A. H. Nielsen, J. Opt. Soc. Amer., 50, 1264 (1960).

14. J. L. Himes and T. A. Wiggins, J. Molec. Spectrosc., 40, 418 (1974).

15. T. Ueda and T. Shimanouchi, J. Molec. Spectrosc., 28, 350 (1968).

16. F. A. Miller and W. G. Fatelely, Spectrochim. Acta, 20, 253 (1964).

17. W. J. Lafferty, A. G. Maki and E. K. Plyler, J. Chem. Phys., 40, 224 (1964).

18. P. R. Bunker and B. M. Landsberg, J. Molec. Spectrosc., 67, 374 (1977).

19. R. L. Redington and K. C. Lin, J. Chem. Phys., 54, 4111 (1971).

20. Y. Marechal and A. Witkowski, J. Chem. Phys., 48, 3697 (1968).

21. L. A. Curtiss and J. A. Pople, J. Molec. Spectrosc., 61, 1 (1976).

22. R. L. Redington and T. E. Redington, J. Molec. Spectrosc., in press.

23. D. F. Smith, J. Chem. Phys., 28, 1040 (1958).

24. J. S. Kittelberger and D. F. Hornig, J. Chem. Phys., 46, 2099 (1967).

25. R. L. Redington, J. Chem. Phys., 44, 1238 (1966).

26. J. Janzen and L. S. Bartell, J. Chem. Phys., 50, 3611 (1969).

27. J. W. Bevan, A. C. Legon, D. J. Millen and S. C. Rogers, J. Chem. Soc. Chem. Comm., 341 (1975).

28. R. K. Thomas, Proc. Roy. Soc. Lond. A., 344, 579 (1975).

29. D. G. Lister and P. Palmieri, J. Molec. Structure, 39, 295 (1977).

30. B. S. Ault and G. C. Pimentel, J. Phys. Chem., 77, 57 (1973).

31. R. W. Long, J. H. Hildebrand and W. E. Morrell, J. Amer. Chem. Soc., 65, 182 (1943).

32. R. L. Jarry and W. Davis, Jr., J. Amer. Chem. Soc., 57, 600 (1953).

33. W. Strohmeier and G. Briegleb, Z. Elektrochem., 57, 662 (1953).

34. J. N. Maclean, F. J. C. Rossotti and H. S. Rossotti, J. Inorg. Nucl. Chem., 24, 1549 (1962).

35. J. H. Hu, D. White and H. L. Johnston, J. Amer. Chem. Soc., 75, 1232 (1953).

36. E. U. Franck and F. Meyer, Z. Elektrochem., 63, 571 (1959).

37. C. E. Vanderzee and W. W. Rodenburg, J. Chem. Thermodynamics, 2, 461 (1970).

38. J. O. Hirschfelder, C. F. Curtiss and R. B. Bird, "Molecular Theory of Gases and Liquids", John Wiley & Sons, New York, N. Y. (1954).

39. S. Murad, QCPE 10, 357 (1978).

40. W. L. Jorgensen and M. E. Cournoyer, J. Amer. Chem. Soc., 100, 4942 (1978).

41. A. Karpfen and P. Schuster, Chem. Phys. Lett., 44, 459 (1976).

42. W. J. Hehre, W. A. Lathan, R. Ditchfield and J. A. Pople, QCPE 11, 236 (1973).

43. M. Kertesz, J. Koller and A. Azman, J. Molec. Struct., 36, 336 (1977).

44. P. W. Payne, J. Chem. Phys., 65, 1920 (1976).

45. M. Atoji and W. N. Lipscomb, Acta Cryst., 7, 173 (1954).

III. PUBLICATIONS

Each of the three subsections discussed in Section II of this report is being developed into manuscripts to be submitted for publication. Probable titles, authors and journals are:

1. "Infrared Matrix-Isolation Studies of H_nF_n Oligomers" by R. L. Redington and D. F. Hamill; J. Chem. Phys., J. Phys. Chem. or J. Molec. Spectrosc.
2. "Nonideal Gas Model for HF Vapor" by R. L. Redington; J. Phys. Chem. or J. Am. Chem. Soc.
3. "Gaussian Basis Studies of H_nF_n Oligomers" by D. F. Hamill and R. L. Redington; J. Phys. Chem. or Int. J. Quant. Chem.

IV. PERSONNEL

1. Principal Investigator: Richard L. Redington, Professor of Chemistry, Texas Tech University.
2. Research Assistant: Delphia F. Hamill. This research will form a portion of her Ph.D. thesis, to be completed in 1980.

V. MEETINGS

1. "Studies of H_nF_n Oligomeric Species" by R. L. Redington; Air Force Contractors Meeting, U. S. Air Force Academy, Colorado Springs, October, 1979.
2. "Infrared Matirx-Isolation Spectra of H_nF_n Oligomers" by D. F. Hamill and R. L. Redington; Southwestern Regional Meeting of the American Chemical Society, Austin, Texas, December, 1979.

Table I

Infrared Spectrum of Hydrogen Fluoride
Isolated in an Argon Matrix

Ref. 3	Ref. 1	Present work	Assignment/comment
3997	3997 cm^{-1}		monomer, R(1)
3962	3963.0	3962	monomer, R(0)
3953	3954.3	3953	monomer
		3934	
3920	3919.4	3920	chain trimer
	3915.6		
		3904	
	3897.6	3898	
3878	3881.4	3881	dimer
3875	3876		monomer, P(1)
	3867.9		
	3826	3826	chain trimer
		3818	satellite; decrease on annealing
3785		3787	dimer
	3777.2	3774	water monomer
3767			
	3757	3757	water monomer
	3755.2		
	3744.0	3444	water dimer
	3737.7	(3737)	
		(3726)	
	3724.4		
		3718	HF-water; trimer?, OH stretch
		3712	water monomer
	3711.0		
	3702.4	3702	chain trimer
	3697.6	3694	satellite; inc., then dec. on anneal
		3675	
	3669.0	3669	HF-water; trimer?, HF stretch

Ref. 3	Ref. 1	Present work	Assignment/comment
	3637.9 cm^{-1}		
	3656		
	3606	(3601)	
	3596.4		
	3573.3	3573	water dimer
	3556	3554	HF - water trimer
	3530	3533	
	3517		
	3483		
		3428	cyclic tetramer
		3414	
		3403	
	3374		
		3250-60	cyclic hexamer
		753	cyclic hexamer?
		746	satellite
		723	cyclic tetramer?
		716	satellite
		698	increase on annealing
		683	increase on annealing
		636	HF-water, trimer?
		630	HF-water, satellite
		615	HF-water, trimer?
		609	HF-water, satellite
		579	increase on annealing
		561	chain trimer
		499	
		464	increase on annealing
		446	chain trimer
		~402	

Table II.

Some Fundamental Vibrations of H_nF_n Oligomers

		No. IR Modes	HF stretching			No. IR Modes	FH· · ·F bending	
HF	monomer	1	3953,62			0		
H_2F_2	dimer	2	3881	3787		2		
H_3F_3	chain trimer	3	3920	3826	3702	4	561	446
H_4F_4	cyclic tetramer	1			3428	1	723	
H_6F_6	cyclic hexamer	1			3250	1	753	
HFH_2O	dimer	1			3608 (vapor)	2		
$H_2F_2H_2O$	trimer	2	(3718, OH?)	3671?	3554	4	636	615

Table III, Part A

Thermodynamic Properties Calculated for HF Vapor Models*

Oligomerization Enthalpies, kJ/mole

Model	ΔH_2	ΔH_4	ΔH_6
a)	-32.1	-88.0	-172.5
b)	-32.0	-92.8	-172.1

Entropy of Vapor, J/mole·deg

Model	56°C	44°C	38°C	32°C	26°C
a)	78.1	68.2	63.4	59.8	55.9
b)	78.4	68.4	63.8	60.1	56.2
observed	78.7	67.9	65.4	63.1	58.5

Nonideality factor, Z_n, of Saturated Vapor

Model	56°C	44°C	38°C	32°C	26°C
(a)	1.14	1.20	1.18	1.24	1.30
observed	1.35	1.28	1.25	1.26	1.27
(b)	1.21	1.30	1.27	1.39	1.49
observed	1.35	1.28	1.26	1.26	1.28

Monomer Second Virial Coefficients, dm^3/mole

Model	56°C	44°C	38°C	32°C	26°C
(a)	-0.41	-0.73	-0.78	-1.13	-1.53
(b)	-0.58	-1.02	-1.08	-1.61	-2.16

*Models (a) and (b) described in text and also shown in van't Hoff plots of Fig. 3.

Table III, Part B

Vapor Phase Heat Capacity, J/mole·deg

P,kPa	56°C (a)	56°C (b)	56°C obs.	26°C (a)	26°C (b)	26°C (obs.)
15.5	34.1	33.5	35.1	56.3	54.5	53.6
30.7	39.4	38.4	41.8	230	225	218
42.5	44.8	43.5	46.9	590	582	544
50.7	50.0	48.5	54.4	812	807	745
56.0	54.4	52.7	58.6	884	882	866
69.2	70.5	68.5	66.9	839	843	920
83.0	99.3	96.8	105	666	671	820
96.1	142	139	151	520	523	682
101	--	--	--	472	475	623

Oligomer Partial Pressures, kPa

P	56°C P_1 (a)	56°C P_1 (b)	56°C P_2 (a)	56°C P_2 (b)	56°C P_4 (a)	56°C P_4 (b)	56°C P_6 (a)	56°C P_6 (b)	26°C P_1 (a)	26°C P_1 (b)	26°C P_2 (a)	26°C P_2 (b)	26°C P_4 (a)	26°C P_4 (b)	26°C P_6 (a)	26°C P_6 (b)
15.5	15.4	15.4	0.1	0.1	0.0	0.0	0.0	0.0	15.2	15.3	0.2	0.2	0.0	0.0	0.0	0.0
42.5	42.0	42.1	0.5	0.4	0.0	0.0	0.0	0.0	40.0	40.1	1.5	1.4	0.2	0.2	0.9	0.8
56.0	55.1	55.2	0.9	0.8	0.0	0.0	0.0	0.0	50.0	50.2	2.4	2.1	0.4	0.5	3.3	3.2
83.0	81.0	81.2	1.9	1.7	0.1	0.1	0.1	0.1	63.7	64.2	3.9	3.5	1.0	1.2	14.4	14.1
101	-	-	-	-	-	-	-	-	69.9	70.5	4.7	4.2	1.5	1.8	25.2	24.8

Table IV

Optimized Geometries Using STO-3G Basis Set

Coordinate	H_3F_3 ring	H_4F_4 ring	H_3F_3 chain	H_4F_4 chain
FH, r_1	9.59 nm	9.38	9.55	9.56
r_2			9.54	9.55
r_3			9.53	9.57
r_4				9.52
FF, R_1	25.8 nm	23.1	25.0	25.6
R_2			24.7	24.9
R_3				25.3
R_4				
$H_iF_iF_j$ α_1	21.3	9.2	18.6	2.71
α_2			17.9	1.88
α_3				2.36
$F_iF_jH_j$ β_1			109.1	110.0
β_2			100.3	111.6
β_3				111.7
Energy, Hartree	-295.74529	-394.36185	-295.73698	-394.32927
Stabilization energy, kJ	-23.5	-46.4	-24.3	-33.2
Dipole moment, debye	0	0	4.0	6.6

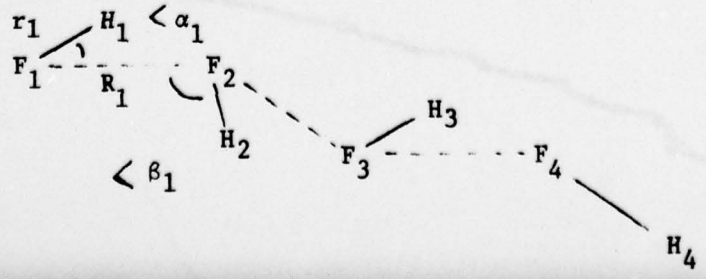

Figure 1A.

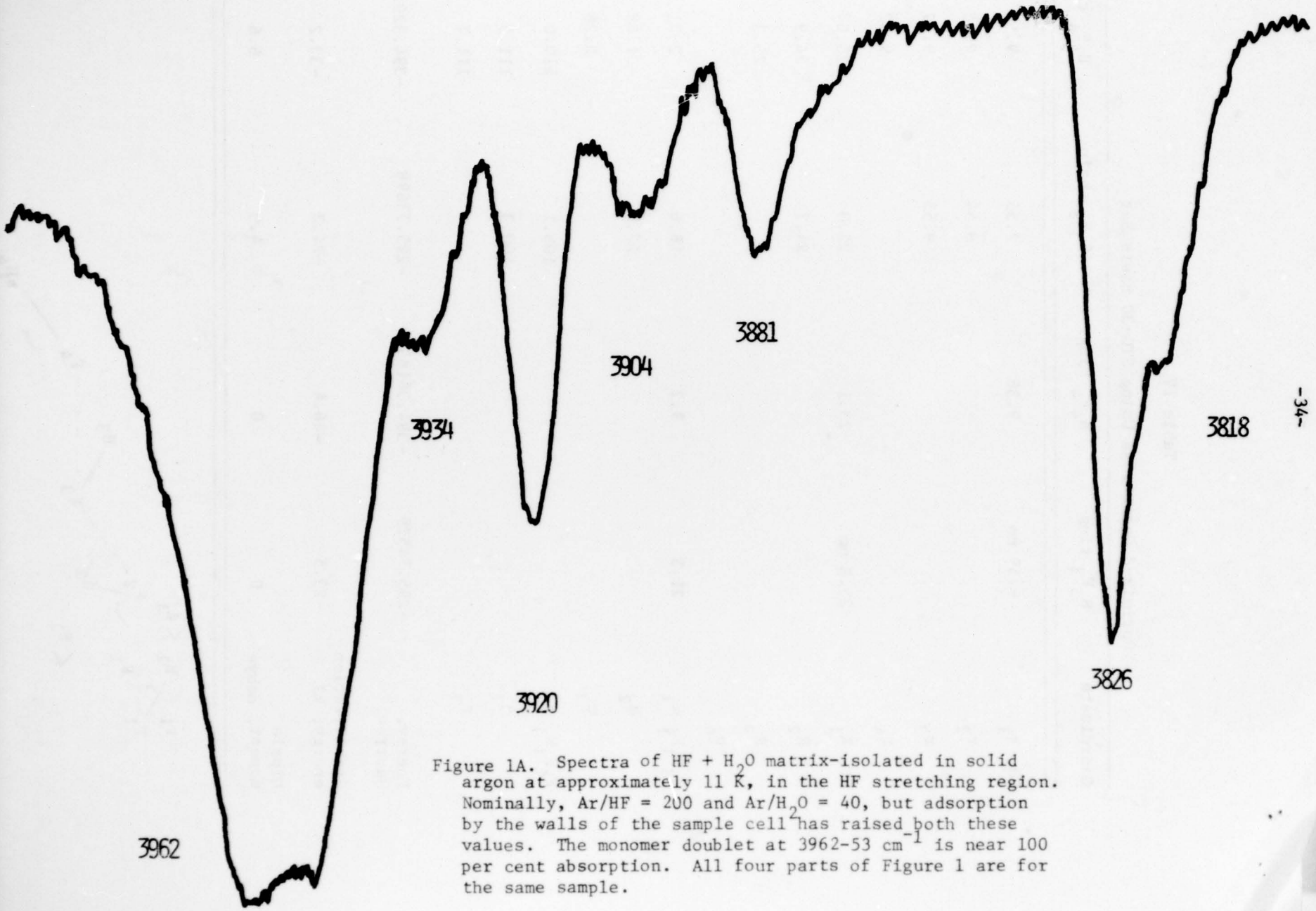

Figure 1A. Spectra of HF + H_2O matrix-isolated in solid argon at approximately 11 K, in the HF stretching region. Nominally, Ar/HF = 200 and Ar/H_2O = 40, but adsorption by the walls of the sample cell has raised both these values. The monomer doublet at 3962-53 cm^{-1} is near 100 per cent absorption. All four parts of Figure 1 are for the same sample.

Figure 1B.

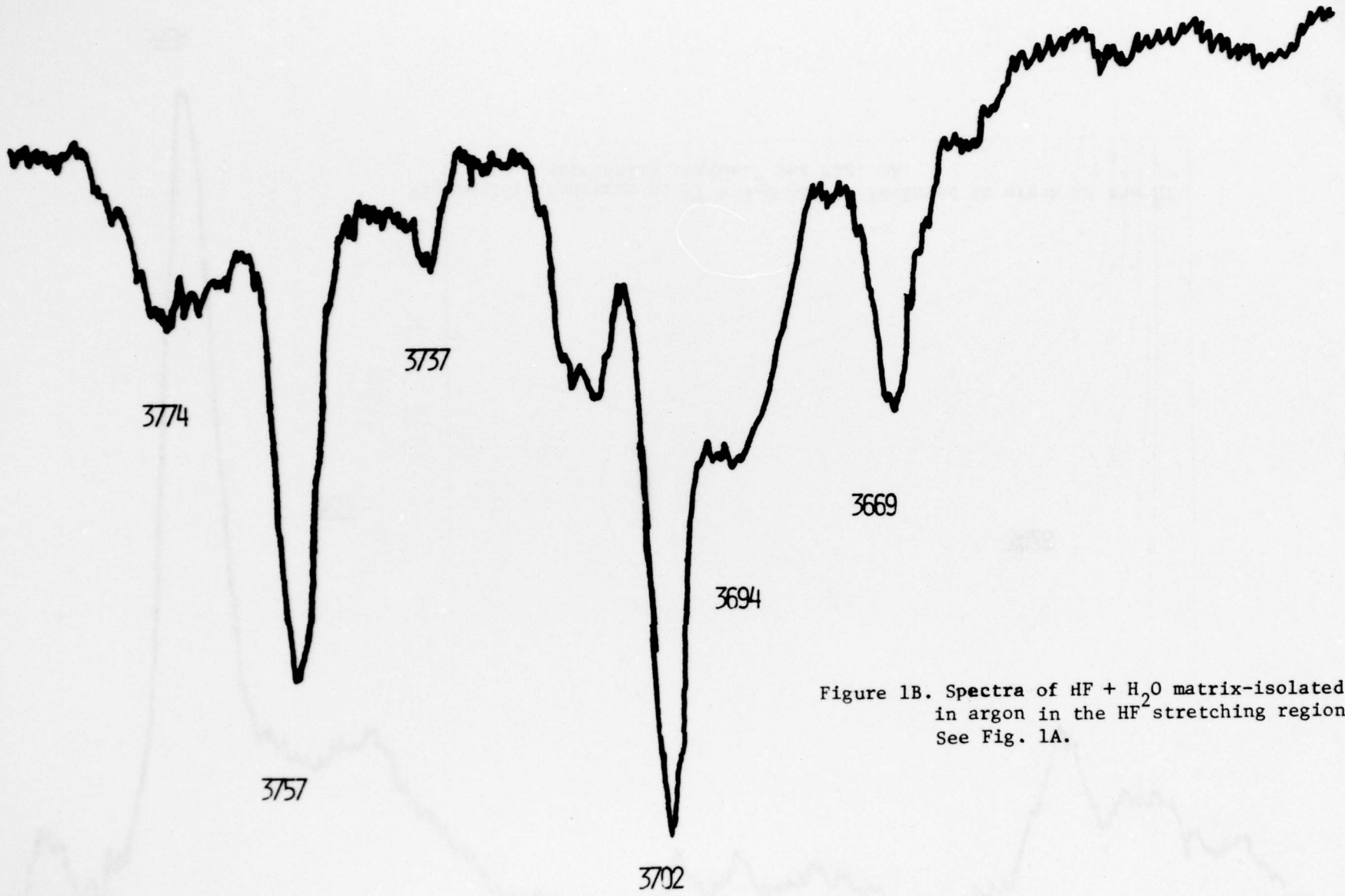

Figure 1B. Spectra of HF + H_2O matrix-isolated in argon in the HF stretching region. See Fig. 1A.

Figure 1C.

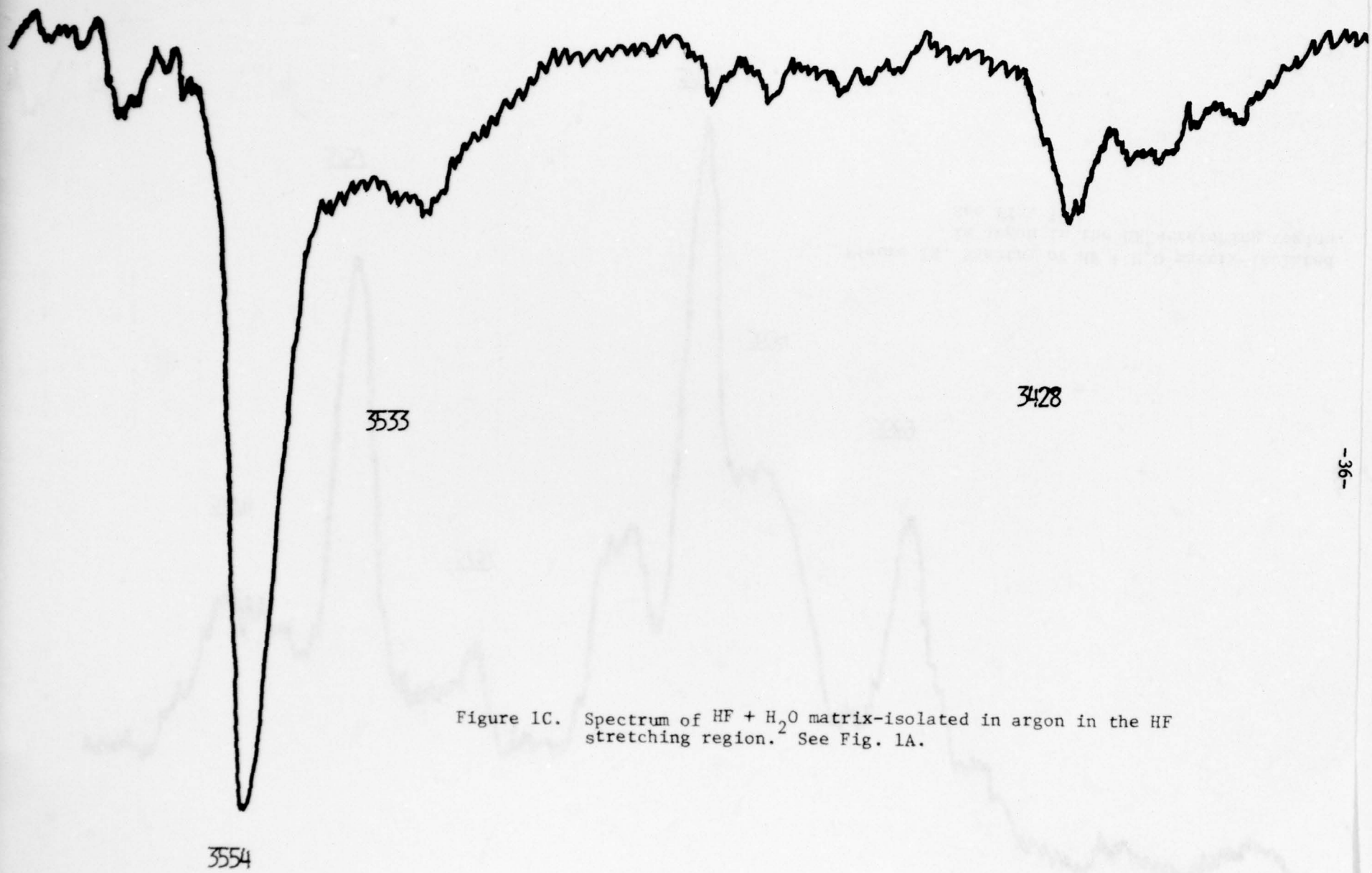

Figure 1C. Spectrum of HF + H_2O matrix-isolated in argon in the HF stretching region. See Fig. 1A.

Figure 1D.

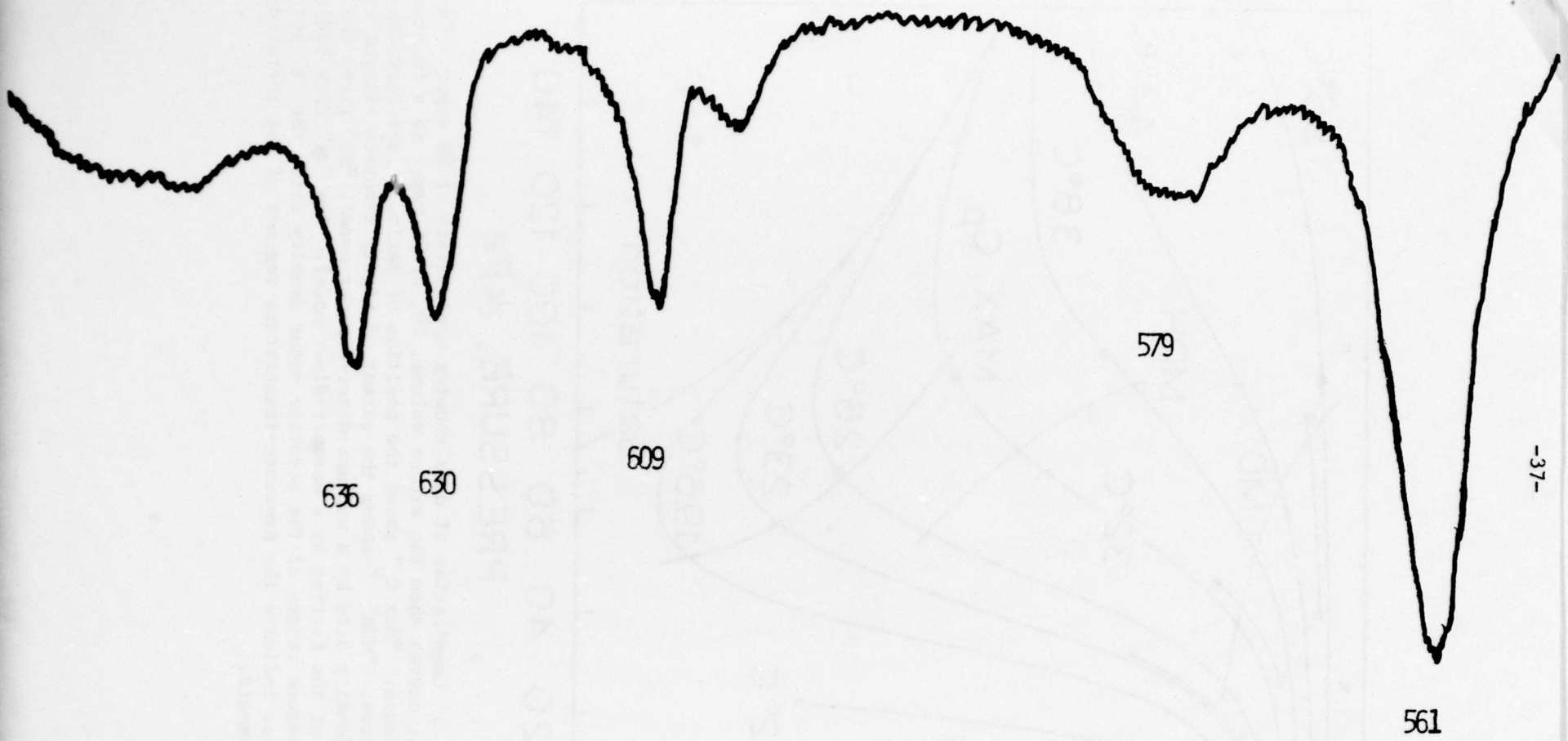

Figure 1D. Spectrum of HF + H_2O matrix-isolated in argon in the FH· · ·F bending region. See Fig. 1A.

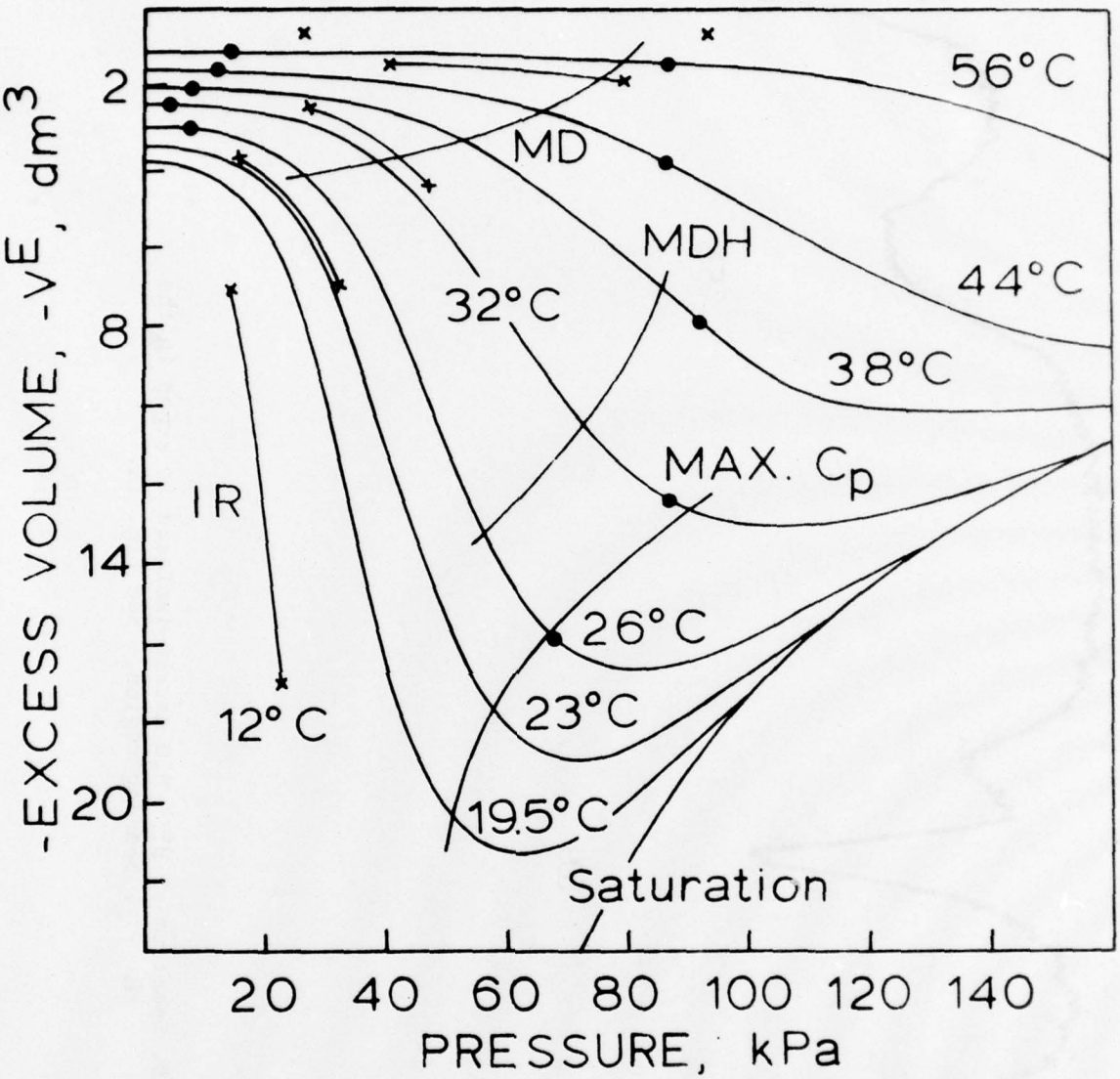

Figure 2. Compilation of data showing nonideality of HF vapor. The dominant curves show the excess volume, V^E, of HF vapor as a function of pressure. "Max C_p" shows the position of maxima in the heat capacity curve. "MDH" shows the extent of highly accurate fitting of vapor density data by a monomer-dimer-hexamer model, "MD" gives the extent of the fitting by a monomer-dimer model. The "●" dots indicate the pressure ranges of the accurate vapor density data; the "x" points and lines indicate the pressure-temperature regimes of the infrared measurements.

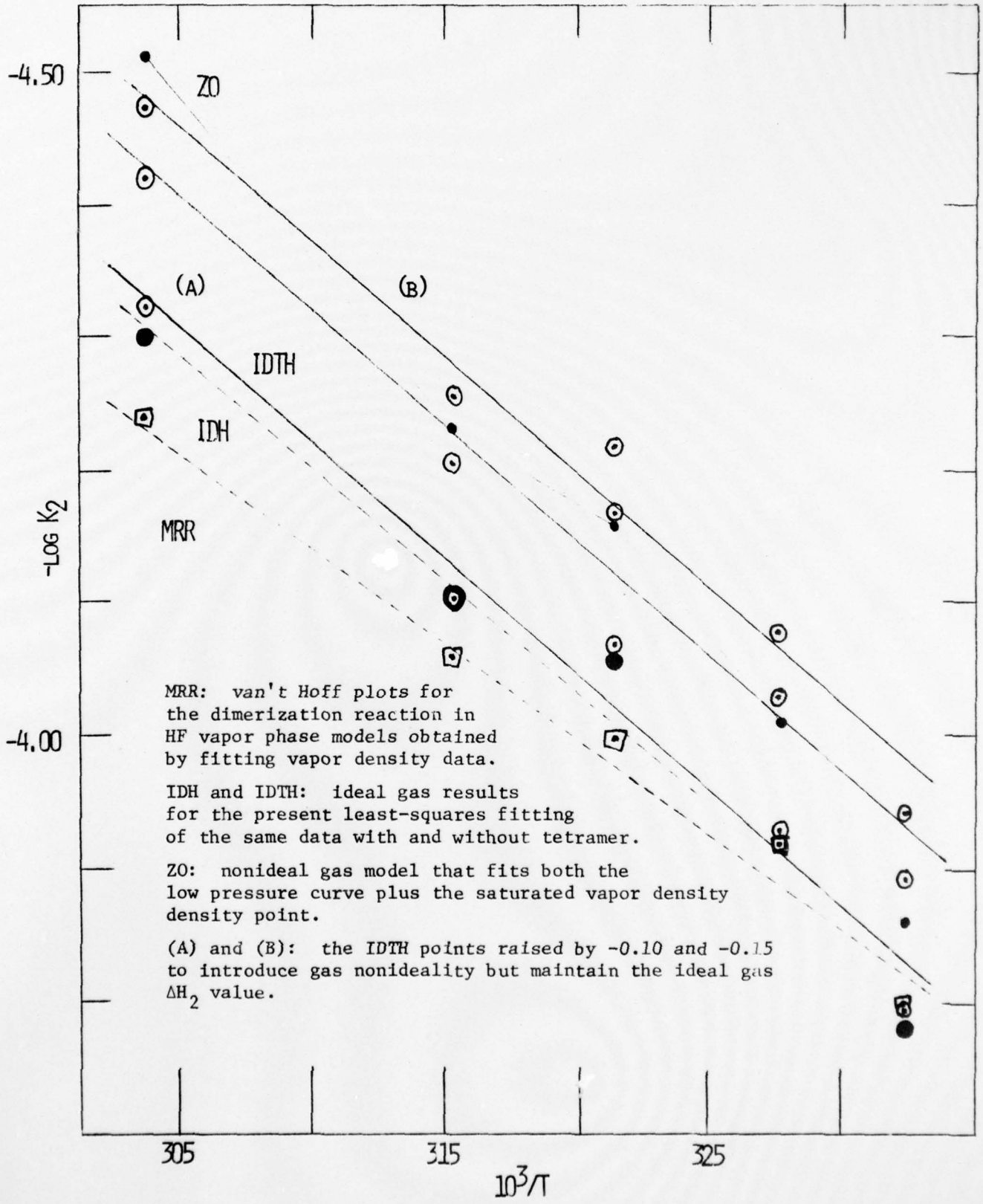

Figure 3. van't Hoff plots for the dimerization reaction in HF vapor phase models obtained by fitting vapor density data.